UNIVERSITY OF CAMBRIDGE

Thermal Conductivity of Soils

By

Guowen Tan (Trinity College)

Fourth-year Undergraduate Project

In Group D, 2011/2012

I hereby declare that, except where specifically indicated, the work submitted herein is my own original work

ACKNOWLEDGEMENT:

I would like to thank Dr Stuart Haigh for his constructive advice and general help offered in the experiments and whole project. I would also like to thank Chris McGinnie and Richard Adams for their help on fixing thermal couples and providing soil samples. Without their help, the project would not be conducted smoothly.

1. ABSTRACT

The thermal properties of soil are a component of soil physics that has been found to be important in diverse areas including engineering, climatology and agriculture, for example, the expansion and contraction of construction materials especially in freezing soils, longevity and efficiency of gas pipes or electrical cables buried in the ground, energy conservation schemes, in agriculture for timing of planting to ensure optimum seedling emergence and crop growth and in measuring greenhouse gas emissions as heat effects the liberation of carbon dioxide from soil. Soil thermal properties are also becoming important in areas of environmental science such as determining water movement in radioactive waste and in locating buried land mines. These properties determine how energy is partitioned in soils. While related to soil temperature, they are more accurately associated with the transfer of heat through soils, by the three main mechanisms: radiation, conduction and convection. There are three main soil thermal properties: volumetric heat capacity with SI units: $Jm^{-3}K^{-1}$, thermal conductivity with SI units: $Wm^{-1}K^{-1}$ and thermal diffusivity with SI units: m^2s^{-1}.

The objective of this project is to investigate the factors that affect thermal conductivity. In coarse materials, significant heat transfer takes place due to convection. The permeability of soils is thus one obvious factor, which affects the apparent thermal conductivity. The first part of the project, particle soil samples with different permeabilities were tested, including Gravels with particle diameters of 10 mm and 5 mm, Fraction A sand, Fraction B sand (Fraction B is finer than Fraction A), Hostun sand and mixtures of these. Another factor is thermal power transmitted through the sample. According to Lapwood (1948), there is a criterion for convective flow: if the temperature gradient is less than a certain value, any disturbance dies away, but when it reaches this value, steady convection becomes possible. Therefore, some of the soil packings were tested with different thermal powers illustrating the threshold effect. In order to compare the relationship between conduction and convection, three dimensionless groups are used: dimensionless thermal conductivity β ________________________________

The first set of experiments involved one-dimensional heat transfer. In the second part of the project, two-dimensional tests were performed using buried pipes. The values of dimensionless groups were calculated and compared in order to quantify the onset of convective heat transfer.

2. INTRODUCTION

Recent developments in renewable technology have led to an increasing interest in finding alternative sources of energy for heating, including the ground. The temperature of the foundation zone is about 10-13 ℃ (Clarke, Agab and Nicholson, 2007), which is about the mean air temperature. It is possible to take advantage of this stable temperature to heat or cool the buildings by circulating a liquid through a closed loop within this region (Figure 1) and passing it through a heat exchanger connected to a circulation system within the buildings. Hence, soil thermal properties are important in designing such systems, which could help in saving energy. Saving energy using underground heating/cooling system is particularly important in UK; the majority of energy consumed in domestic sector is for space heating, which in 2009 represented 61% of total domestic energy consumption, and domestic energy consumption accounted for 32% of total UK energy consumption in 2009, which means, space heating along occupied about 19% of UK's total energy consumption (National Statistics, Department of Energy & Climate Change, 2011). Figure 3 (National Statistics, Department of Energy & Climate, 2011) shows domestic energy consumption by end use in the UK from 1970 to 2009. Oil is one of the most important energy sources, accounting for a large percentage of the world's energy consumption, ranging from a low of 32% for Europe and Asia, up to a high of 53% for the Middle East. Therefore, the transport of crude oil is also important. Pipelines are the most efficient method to transport crude oil and refined products, most crude oil being transported through underground pipelines. Knowing the thermal properties of the surrounding soils is thus essential, since the temperature of oil must be maintained in a certain range. Heat energy will be dissipated through conduction and convection between pipelines and soils. In this case, heat loss of the pipelines must be minimized, to prevent waxing of the oil leading to flow problem or excessive energy consumption, which increases the transportation cost. Figure 2 (Pacific Northwest National Laboratory, 2009) shows an example of an underground oil pipeline. Soils' thermal properties are also important in many other areas such as agriculture, determining the optimum time for seeding.

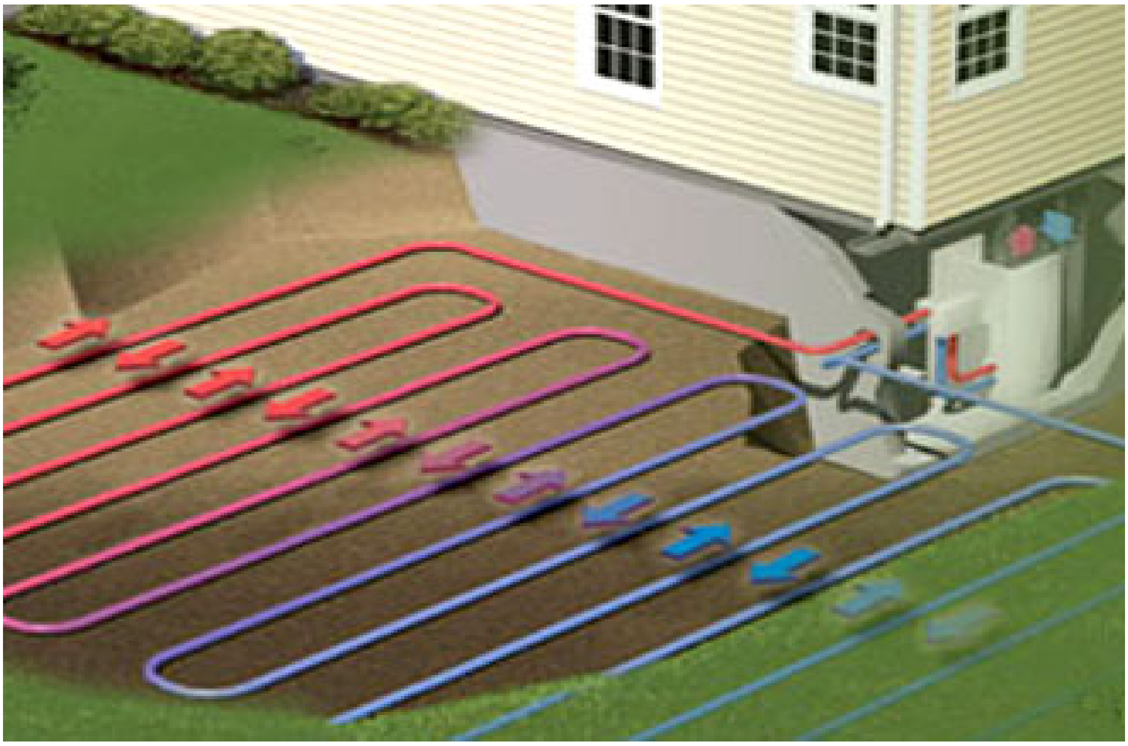

Figure 1. Underground Heating/Cooling System (Home Footprint, 2012)

Figure 2. Underground Oil Pipeline

(Pacific Northwest National Laboratory, 2009)

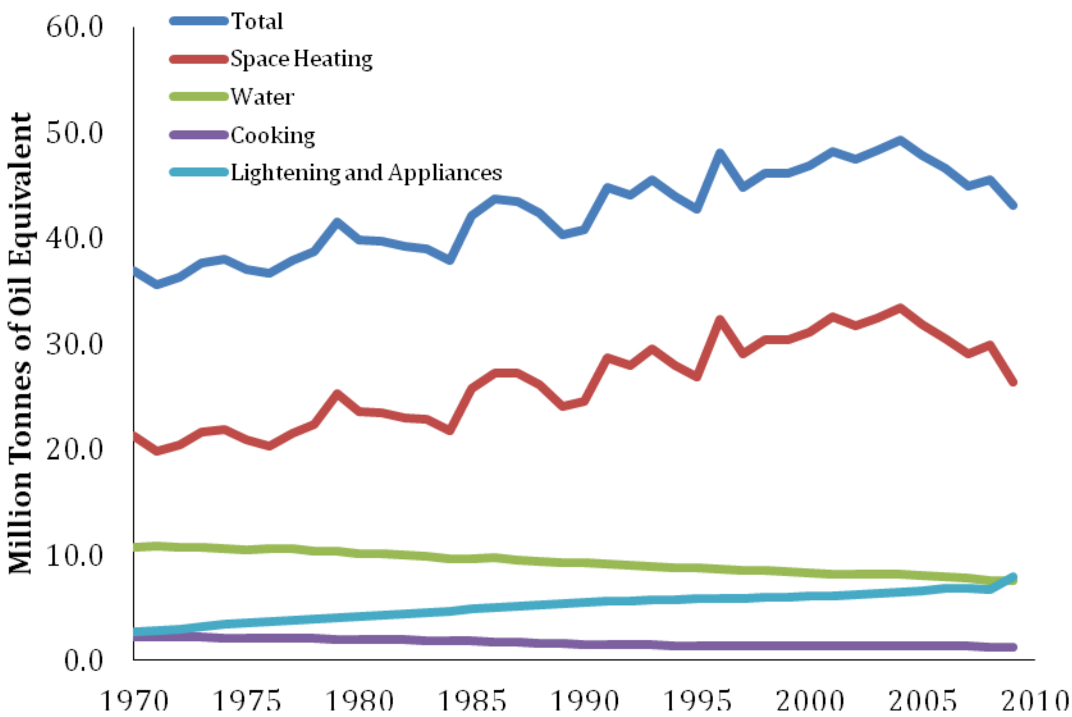

Figure 3. Domestic Final Energy Consumption By End Use, UK, 1970 to 2009

(National Statistics, Department of Energy & Climate, 2011)

3. BACKGROUND AND THEORIES

In this section some background, basic concepts and theories of soil thermal properties will be presented, including modern studies of soil thermal properties, the structure of soils and various heat transfer mechanisms. This section also explains how to predict a soil thermal properties if its composition is known as well as modern measurement techniques.

3.1 MODERN STUDIES OF SOIL THERMAL PROPERTIES

A quantified understanding of soil thermal properties is of great importance in the study of global energy and water cycles as well as to many industrial processes. A lot of attention has been drawn to the examination of energy partitioning and budget (Kim *et al*., 2000) and the hydrological cycle (Nagai, Kobayashi and Ishikawa, 2000), however, little research has been done regarding soil's thermal properties. In this section, some modern studies of soil thermal properties are presented. Areas of concern of soil thermal properties include thermal conductivity, thermal diffusivity and volumetric heat capacity. Volumetric heat capacity could be easily determined according to soil composition (Van Wijk, 1963). Both thermal conductivity and thermal diffusivity are related to volumetric heat capacity; hence, only one of them needs to be determined. Soil heat transfer is caused by a complex combination of conductive and convective processes (Passerat de Silans, Monteny and Lhomme, 1996). Passerat considered soil thermal diffusion as a bulk motion, which was assimilated to a conductive process. Different methods of determining soil thermal conductivity and diffusivity have been published. Some based on theoretical models (De Vries, 1963) or semi empirical models (Johansen, 1975). Most resulted from the analytical solution of the one-dimensional thermal conduction and convection equation, which could be solved analytically by applying the traditional harmonic method (HM) and the Laplace transform method (LTM). Horton, Wierenga and Nielsen (1983) examined several of these methods and showed that the Harmonic method is more reliable than the other methods because the analytical method used in these models does not require knowledge of the initial temperature profile. Methods based on Laplace Transform are also used, but require a constant initial temperature profile

(Kavianipoor and Beck, 1977; Asrar and Kanemasu, 1982). Passerat de Silans, de Silans, Monteny and Lhomme (1996) summarized these studies and examined them with data from the HAPEX-Sahel experiment, and the result showed that both HM and LTM could be used to obtain apparent soil diffusivity from a measured soil temperature profile with the aid of the least-square method (Gao, Fan and Bian, 2003).

Shao, Horton and Jaynes (1998) compared the results from the analytical solution with the data from a field infiltration experiment with natural temperature variations and found good agreement. Ren, Kluitenburg and Horton (2000) presented a method to determine soil water flux and pore water velocity by a heat-pulse technique, which improved earlier methods by reducing distortion of the water flow field and minimizing heat-induced soil water redistribution.

3.2 STRUCTURE OF SOILS

In order to understand the effects of various heat transfer mechanisms on soil's thermal properties, it is essential to understand soil structure. Soils are often treated as a three-phase system since they can be thought as mixtures of soil particles, water and air. Capillary bridges of water connect soil particles with air bubbles in between. Figure 4 shows an idealised soil structure.

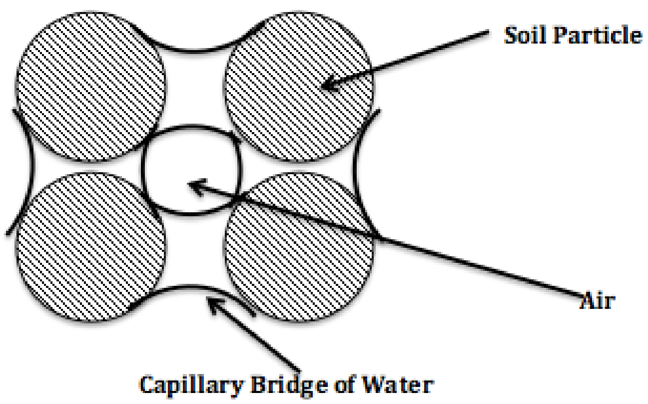

Figure 4. Idealised Soil Structure

The amounts of air and water in soils can greatly affect their thermal properties. This is quantified by voids ratio and volumetric water content. Voids ratio can be calculated from the volume of the solid phase using:

$$e = \frac{V_v}{V_s} = \frac{V_v}{V_T - V_v} = \phi \frac{\square}{1 - \phi} \qquad (1)$$

e is voids ratio;

V_{void} is the volume of void-space (air and water);

V_s is the volume of solids;

V_T is the total volume, including volumes of solids, water and air

n is porosity and is defined as:

$$n = \frac{V_{void}}{V_T} \qquad (2)$$

Volumetric water content is defined as:

$$\theta = \frac{V_w}{V_T} \qquad (3)$$

V_w is the volume of water

The relative humidity is also an important parameter, since it determines the magnitude of moisture dependent water vapour diffusion:

$$\varphi = \frac{P_w}{P_w^*} \qquad (4)$$

P_w is the partial pressure of water vapour in the air-water mixture and P_w^* is the saturated vapour pressure of water at a given temperature.

3.3 HEAT TRANSFER MECHANISMS

Heat transfer in moist and porous media can be influenced by a number of different mechanisms. In addition to heat conduction, these include thermal radiation, convection and water vapour diffusion.

3.3.1 RADIATION

Radiation is a process in which energetic particles or energetic waves travel through a medium or space. Two types of radiation are commonly differentiated in the way they interact with normal chemical matter: ionizing and non-ionizing. This project involves thermal radiation, which is a type of non-ionizing radiation. Thermal radiation, a common synonym for infrared, is the process by which the surface of an object radiates its thermal energy in the form of electromagnetic waves. Thermal radiation is generated when heat from the movement of charged particles within atoms is converted to electromagnetic radiation. The frequency of the emitted waves is a probability distribution dependent on temperature only. In the case of heat transfer in soils, the magnitude of thermal radiation is positively proportional to pore area and temperature. Generally, the effect of radiation is small compared to other heat transfer mechanisms, especially conduction. Even for a particle diameter of 20 *mm*, the effect of radiation amounts to no more than 10% of total heat conduction at normal atmospheric temperature, while in sand (particle diameters below 2 *mm*), the effect is less than 1% (Johansen, 1977). In this calculation, the porosity is assumed to be $n = 0.395$, which corresponds to a dry density for sand of about $1600\ ^{kg}/_{m^3}$. The effect of radiation will be even less for higher density soils and completely insignificant in moist materials. Above all, this shows the thermal radiation is negligible in moist soils and could only play a role in coarse, crushed stone materials. Although the effect of thermal radiation could be incorporated in equivalent heat conductivity, it is ignored in this project for simplicity.

3.3.2 CONDUCTION

In heat transfer, conduction is a mode of transfer of energy within and between bodies of matter, due to a temperature gradient. Conduction means collisional and diffusive transfer of kinetic energy through particles of ponderable matter (as distinct from photons). Conduction takes place in all forms of ponderable matter, such as solids, liquids, gases and plasmas. Heat spontaneously tends to flow from a body at a higher temperature to a body at a lower temperature. In the absence of external driving fluxes, temperature differences, over time, approach thermal equilibrium. In solids, it is due to the combination of vibrations of the molecules in a lattice or phonons with the energy transported by free electrons. In gases and liquids, conduction is due to the collisions and diffusion of the molecules during their random motion. If there is no heat transfer via currents in the liquid, conduction will be the most significant heat transfer mechanism compared to others.

3.3.3 CONVECTION

Convective heat transfer is a mechanism of heat transfer occurring because of bulk motion (observable movement) of fluids. Steady convection is not always possible under one-dimensional condition. According to Lapwood (1948), there exists a threshold value of temperature gradient for steady convection to become possible; he examined the breakdown of stability of a layer of fluid subject to a vertical temperature gradient in a porous medium and the possibility of convective flow.

Heat is the entity of interest being advected (carried), and diffused (dispersed). This can be contrasted with conductive heat transfer that is the transfer of energy is by vibrations at a molecular level through a solid or fluid, and radioactive heat transfer, the transfer of energy through electromagnetic waves. There are three types of convection: natural convection, forced convection and gravitational or buoyant convection. Natural convection occurs due to temperature differences, which affect the density. Therefore, heavier components will fall, while lighter components rise, leading to bulk fluid movement. Force convection is the fluid movement results from external surface force such as a fan or pump, which is typically used to increase the rate of heat exchange. Gravitational convection is a type of natural convection induced by buoyancy variations resulting from material properties other than temperature. Typically this is caused by a variable composition of the fluid. For low velocity flows, the temperature differences between liquid and particles will be small and the convection between them could be neglected. There are two dimensionless numbers associated with heat convection: Nusselt number Nu and Rayleigh number Ra. In heat transfer at a boundary within a fluid, the Nusselt number is the ratio of convective to conductive heat transfer across the boundary. If a Nusselt number is close to one, it means convection and conduction are of similar magnitude, a large Nusselt number corresponds to more active convection while a small Nusselt number shows conduction dominates. Nusselt number is defined as:

$$Nu = \frac{convectiove\ heat\ transfer\ coefficient}{conductive\ heat\ transfer\ coefficient}$$

$$\Rightarrow Nu = \frac{total\ heat\ transfer\ coefficient - conductive\ heat\ transfer\ coefficient}{conductive\ heat\ transfer\ coefficient}$$

$$\Rightarrow Nu = \frac{total\ heat\ transfer\ coefficient}{conductive\ heat\ transfer\ coefficient} - 1 \qquad (5)$$

In fluid mechanics, the Rayleigh number is a dimensionless number associated with free convection flow and is a quantity used to compare the amount of convection and conduction in a fluid. When the Rayleigh number is below a critical value, heat transfer is primarily in the form of conduction; when it exceeds the critical value heat transfer is primarily in the form of convection. According to Johansen (1977), Rayleigh number could be defined as:

$$Ra = \frac{\alpha g H k \Delta T}{\kappa \nu} \qquad (6)$$

α is the volumetric thermal expansion coefficient of water, and the value is 0.000207 K^{-1}

g is the gravitational acceleration with value 9.8 ms^{-2}

k is permeability with units: ms^{-1}

ΔT is the temperature difference with units: K

κ is diffusivity with units: m^2s^{-1}

ν is kinematic viscosity of water with units: m^2s^{-1}

Since $\kappa = \frac{\lambda}{C_p}$, where λ is thermal conductivity and C_p is volumetric heat capacity. Therefore:

$$Ra = \frac{C_p \alpha g H k \Delta T}{\lambda \nu} \quad (7)$$

If we assume C_p, α, g and ν are all constants, then we have:

$$Ra = Constant \times \frac{H k \Delta T}{\lambda} \quad (8)$$

The above dimensionless groups will be used as the main parameters in comparing the thermal properties of various soils.

3.3.4 WATER VAPOUR DIFFUSION

Water vapour diffusion is generated due to the variations of water partial pressure in the pores of soils and will be in the direction of falling pressure. Both volumetric water content and temperature could affect the magnitude of water vapour diffusion.

The contribution due to moisture dependent diffusion will be quite small except for the lowest values of water content where the values of relative humidity φ in equation (4) fall significantly below one.

The contribution due to temperature dependent diffusion will decrease when relative humidity starts to fall due to low volumetric water content. It also decreases when water content increases, since the pores are to a large extent filled with water. Water vapour diffusion will contribute to the heat transfer in the form of latent heat exchanged during vaporization and condensation. Since the same temperature field in the pore air controls the temperature dependent vapour diffusion as thermal conduction, it is possible to include the contribution to the heat transfer in the apparent thermal conductivity. The vapour pressure gradient due to a temperature gradient is given by equation (9) below:

$$\nabla P_W = \varphi \frac{dP_W^*}{dT} \nabla T \quad (9)$$

According to Fick's law, the amount of heat diffused by vapour is given by:

$$q_v = \frac{D_a}{RT} \varphi \frac{dP_W^*}{dT} \quad (10)$$

While the amount of transported heat is:

$$q = rq_v \qquad (11)$$

And r is the latent heat due to vaporisation of water, equivalent to $2450\ {}^{kJ}/_{kg}$ at $20\ ℃$. D_a is the water vapour diffusion coefficient in air with units: ${}^{m^2}/_{s}$,

Therefore, the contribution of vapour diffusion to the air conductivity is given by equation (12) (Johansen, 1977):

$$\lambda_v = \varphi \frac{rD_a}{RT} \frac{dR_w^*}{dT} \qquad (12)$$

Krischer and Esdorn (1940) determined the vapour diffusion coefficient to be:

$$D_a = \frac{0.244}{P_0} \left(\frac{T}{273}\right)^{2.8} \qquad (13)$$

P_0 is the total pressure in bar, and T is the absolute temperature.

The apparent air conductivity λ' is given by:

$$\lambda' = \lambda_a + \lambda_v \qquad (14)$$

And λ_a is the conductivity of air, and λ_v is the conductivity of water vapour.

From equation (9) we can see that the water vapour pressure increases exponentially with temperature, hence, the volumetric water content rises rapidly with temperature, which means λ_v will also increases dramatically with temperature. This relationship is a major contribution to the increase in conductivity with increasing temperature for moist soil materials. This result can be proved by measurements of thermal conductivity performed by Philip and De Vries (1957) on sand at various temperatures. For both extremely high and low saturation levels, where the thermal vapour diffusion is limited, the dependence on temperature is weak; from low to moderate saturation levels the dependence is strong and thermal diffusion is significant.

3.3.5 CAPILLARY WATER TRANSPORT

If a soil, where humidity is evenly distributed at the outset, is subjected to a temperature gradient, water vapour diffusion will give rise to a transport of moisture in the direction of falling temperature (Johansen, 1977). In a closed system, this will result in a increasing of humidity on the cold side and drying out on the warm side. This result has been demonstrated by many experiments (Rollins et al., 1954, Cary, 1965, Krischer, 1934, Smith, 1939, Joshua and De Jong, 1973). This results a moisture content gradient, which forms a possibility for capillary water transport in a direction opposite to that of the vapour diffusion caused by temperature (since water vapour diffusion happens from high temperature to low temperature). The magnitude of capillary water transport depends on both the moisture content of the soil and its permeability.

3.4 EFFECTS OF VARIOUS HEAT TRANSFER MECHANISMS

Both theoretical and experimental studies of heat transport in moist, porous materials show that the effects of various heat transfer mechanisms depend on the particle size of the materials, the degree of saturation and the temperature. These factors can be utilized to determine limits for the effects of each mechanism. Figure 5 (Johansen, 1977) shows regions of influence for the possible heat transfer mechanisms in different soils.

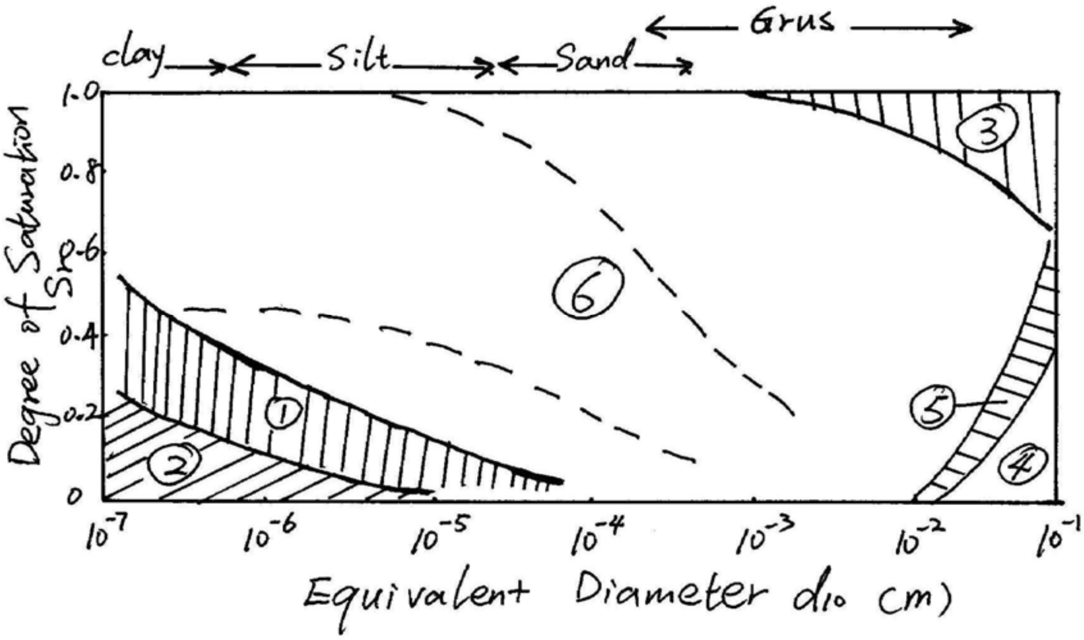

Figure 5. Regions Of Influence For The Possible Heat Transfer Mechanisms In Different Soils. (Figure 23 in Johansen, 1977)

1: Temperature-dependent moisture migration;

2: Moisture-dependent vapor diffusion

3: Convective heat transfer in water

4: Convective heat transfer in air

5: Radiation of heat in voids

6: Heat transfer by conduction

It can be seen that for most materials, conduction will dominate. For fine soil materials such as silt and clay, there is a region (Region 2 in Figure 5) at lower saturation levels, where in this region moisture content gradients will cause vapor diffusion due to change in relative humidity in the pore air as a function of water content and large variations of relative humidity as a function of water content only occur at low saturation levels. For moderate saturation levels in this region, temperature gradients will also cause vapor diffusion in the pore air. For relatively low saturation levels in region 2, the process of vapor diffusion is slow due to low relative humidity values. For relatively high saturation levels, the redistribution of water caused by diffusion is cancelled by capillary water transport in the opposite direction. In section 3.3.5, it was the mentioned that the magnitude of capillary water transport is determined by moisture content of soil and its permeability. Permeability is strongly dependent on the size of the particle and volumetric water content. As the materials become finer, the permeability of soils will decrease, hence the effect of capillary water transfer will become less significant, which means that the redistribution of moisture due to vapor diffusion will become more significant, therefore, the region will move towards higher saturation levels. This effect is shown in region 2.

Temperature dependent vapor diffusion will also contribute to heat transport during the processes of vaporization and condensation. However, since the same temperature field as thermal conduction in the pore air controls the temperature dependent vapour diffusion, thus its contribution can be treated as an added thermal conductivity, which corresponds to region 1 in Figure 5.

For materials with larger particle sizes and relatively low saturation levels, heat transfer is influenced by convection in air (Region4), while for high saturation levels; heat transfer is influenced by convection in water (Region 3).

Radiation (Region 5 in Figure 5) between particles could also contribute to heat transfer in coarse materials, and the contribution is proportional to particle size. Reduced pore cross-section area and increase in conductivity tend to reduce the contribution of thermal radiation in moist soils. The effect of radiation could also be included in the effective conductivity, but the temperature dependence of the parameters must be taken into account, which requires knowledge of the effect of radiation in soil structures.

As conduction dominates for most soils, this is typically assumed in design. In coarse materials, convection may cause an increase in the "apparent" thermal conductivity.

3.5 PREDICTIONS OF SOIL THERMAL PROPERTIES

There are several different approaches to determine soil thermal properties including laboratory tests, empirical fits to databases and analytical models.

A modern laboratory specification to determine the thermal properties of soils involves methods based on measuring the power needed to create a constant temperature difference; on applying a constant power and measuring the resulting temperature difference or on monitoring the temperature change during a transient process. A typical example would be the cylindrical specimens test designed by Clarke (2007), where the ends of a specimen are maintained at different temperatures and heat is allowed to flow axially through the specimen. Tests must be carried out in a constant temperature laboratory or be insulated from background temperature changes. Figure 6 (Clarke, 2007) shows principal features of the laboratory equipment. The method shown in Figure 6 is very similar to the one-dimensional cylinder tests described in section 4.2.2.

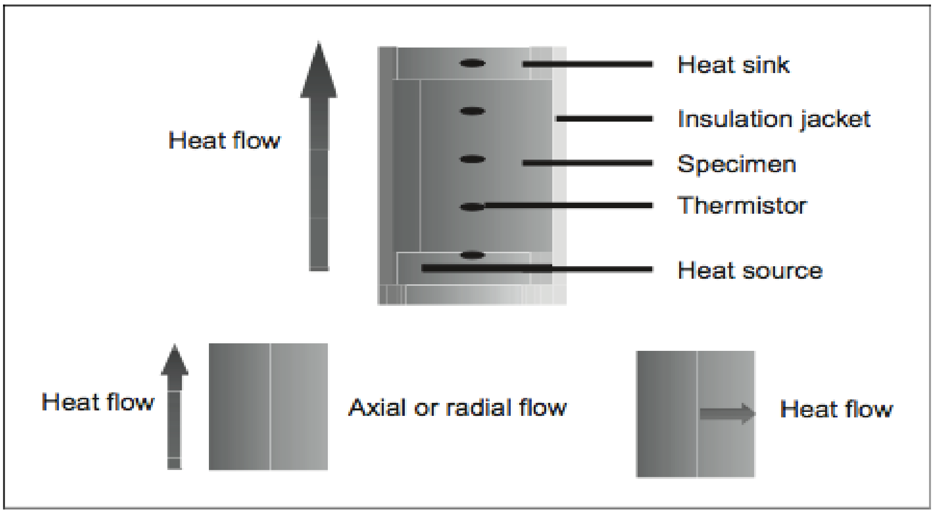

Figure 6. Principal Features of Laboratory Equipment (Clarke, 2007)

While most attempts in predicting soil thermal properties have been based on empirical fits to databases, a few researchers focused on the micro-scale behaviours behind these empirical relationships. Ewing and Horton (2007) examined the thermal conductivity of a cubic lattice of spheres with capillary bridges. However, since the analysis is numerical, this did not show any expression for the thermal conductivity of the lattice. Gemant (1950) developed an analytical solution to predict the thermal conductivity of soils; his analysis is constrained to a single void ratio of 0.9 and saturation ratios between 0 and 0.54, however, the analysis does not capture the correct relationship between thermal conductivity and saturation level, therefore, significantly overestimating the rate of increase of thermal conductivity. Other analytical methods have also been introduced; De Vries (1963) used a model based on Maxwell's equation, but the weighting factor he assumed imply a needle-like shape for the soil particles, unlike normal particles and make the model not very useful.

Haigh (2012) presented a theoretical analysis based on conduction through a simple soil element containing three phases: soil particles, pore water and air. And the method has been shown to be better than the best empirical models in predicting thermal conductivities in a wide variety of sands. The method represents both the physical geometry of the three-phase system and the measured thermal conductivities of a variety of soils. Figure 7 (Haigh, 2012) shows the comparisons of different prediction methods with experimental data for $n = 0.472$ from Chen (2008)

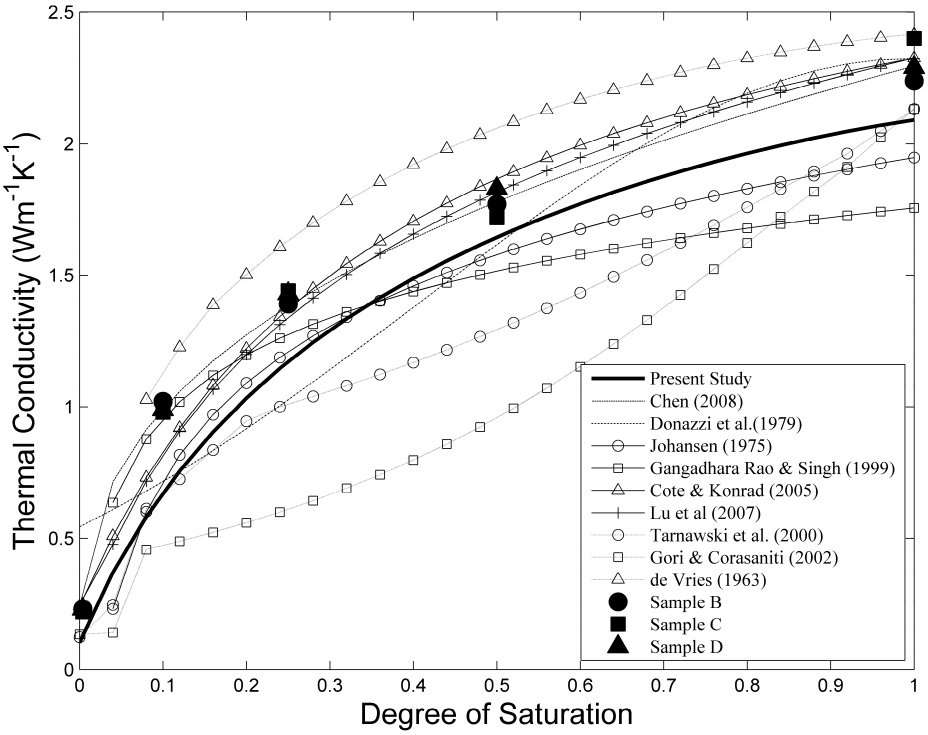

Figure 7. Comparison of Prediction Methods With Experimental Data For $n = 0.472$ from Chen (2008) (Haigh, 2012)

Table 1 (Haigh, 2012) shows the linear regression fits of different prediction methods, the smallest standard error shows that the method provided by Haigh (2012) is the most accurate method of predicting thermal conductivity.

Table 1: Linear Regression Fits Comparing Predicted and Measured Thermal Conductivities

	Gradient	R^2	Standard Error (W/mK)	Number of data points
Present study	1.00	0.86	0.24	151
Chen (2008)	0.92	0.85	0.29	155

Lu et al. (2007)	0.98	0.78	0.32	150
Côté and Konrad (2005)	1.00	0.70	0.32	155
Gori & Corasaniti (2002)	1.17	0.79	0.31	155
Tarnawski et al (2000)	1.28	0.54	0.38	155
Gangadhara Rao & Singh (1999)	1.13	0.77	0.31	131
Donazzi et al. (1979)	1.00	0.73	0.38	155
Johansen (1975)	0.96	0.65	0.32	130
De Vries (1963)	0.89	0.78	0.29	125

4. MODERN MEASUREMENT AND EXPERIMEANTAL TECHNIQUES TO DETERMINE SOILTHERMAL PROPERTIES

It is impossible to give standard numbers soils' thermal properties as they strongly influenced by factors including soil volumetric water content, temperature variations, and volume fraction of solids and air. Air is a poor thermal conductor and reduces the effectiveness of the solid and liquid phases to conduct heat. While the solid phase has the highest conductivity it is the variability of soil moisture that largely determines thermal conductivity. Temperature variations are most extreme at the surface of the soil and these variations are transferred to sub surface layers but at reduced rates as depth increases. Additionally there is a time delay as to when maximum and minimum temperatures are achieved at increasing soil depth. Therefore, being able to measure the thermal properties of soil at a given location becomes crucial. In this section, both modern measurement techniques and experimental techniques used in the project will be introduced.

4.1 MODERN MEASUREMENT TECHNIQUES

The most common techniques used to measure soil thermal properties are using single and dual heat probes and remote sensing. Depending on the objectives, different techniques will be used. The Single and dual heat probes methods are more appropriate in small-scale measurements, when soil thermal properties need to been determined at different locations on a site. Remote sensing involves using satellites and aircraft to measure the thermal properties of the topmost layers of soil at a relatively large scale.

4.1.1 SINGLE AND DUAL HEAT PROBES

The single probe method employs a heat source inserted into the soil and heat is being applied continuously at a given rate. The temperature response adjacent to the heat source will be analyzed via a thermal sensor, thus the thermal properties of the soil could be determined. The method shows the rate at which heat is conducted away from the probe. The main drawback of this technique is that it measures conductivity only. In order to measure other thermal properties including thermal diffusivity and volumetric heat capacity, the dual-probe heat-pulse technique was developed. This consists of two parallel needle probes separated by a certain distance. One probe contains a heater and the other contains a temperature sensor. The device is inserted into the soil, a heat pulse is applied and the sensor records the temperature response as a function of time, which means, a heat pulse is sent from the probe to the sensor at a certain distance away. In such a way, both thermal diffusivity and volumetric heat capacity can be measured and thermal conductivity could be calculated from the other two parameters. Hence, all three main soil thermal properties could be determined. Figure 8(a) and Figure 8(b) (Bristow *et al.*, 2001) show single and dual heat probes:

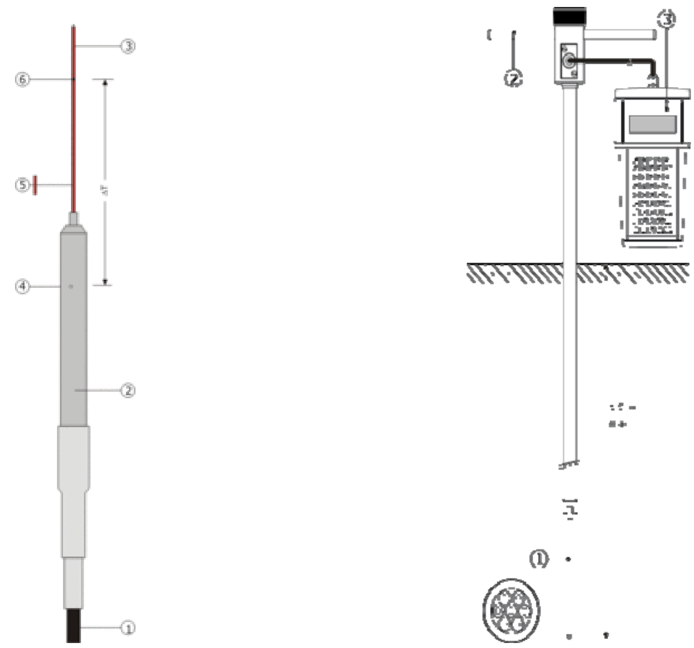

(a) **(b)**

Figure 8: (a) Single Heat Probe, (b) Dual Heat Probe (Bristow *et al.*, 2001)

Figure 8 (a) shows a single heat probe, which consists a needle (3) with a single thermocouple junction (6) and a heating wire (5). It is inserted into the medium that is investigated. Figure 8 (b) shows a dual heat probe, which is an example of a complete system for measurement of soil thermal conductivity, specially designed for measurements at around 1.5 *m* below the surface, which is the typical depth of burial for high voltage cables. When measuring, both single and dual heat probes assume pure thermal conductivity; the effects of other transfer mechanisms will be ignored.

4.1.2 REMOTE SENSING

In the remote sensing method, satellites and aircraft are used to detect the thermal variations of soils. The reflected light from the soil surface indicates the thermal response of the top layers of soil; the infrared wavelength provides energy variations extending to varying shallow depths below the ground surface, which are of most interest. Variations in heat transfer into and out of near surface layers can be detected by thermal sensors because of external heating by the thermal processes of conduction, convection and radiation.

4.2 EXPERIMENTAL TECHNIQUES

This project is divided into two parts: one-dimensional cylinder tests and two-dimensional buried pipe tests. In one-dimensional cylinder tests, the problem is assumed to be one-dimensional since the test cylinders are insulated by foam and heat can only be transferred in the vertical direction. In the second part of the project, a cartridge heater is buried in various soil samples and the cross-sectional temperature variation is examined. In both parts of the experiments, the permeability of soil samples must be calculated first, as it is needed in the calculation of Rayleigh number.

4.2.1 CALCULATION OF SOIL PERMEABILITY

The method used in this project is a simplified version of a falling head permeability test. Soil samples are filled to a certain height in a measuring cylinder, in this case, the height of the samples is fixed to 0.1 *m*. Both ends of the samples are marked and the time for the water surface to fall by a fixed distance is recorded. Permeability is calculated using the formula below. Several measurements are made to improve accuracy. Figure 9 shows a systematic view of permeability test apparatus and the derivation of the formula:

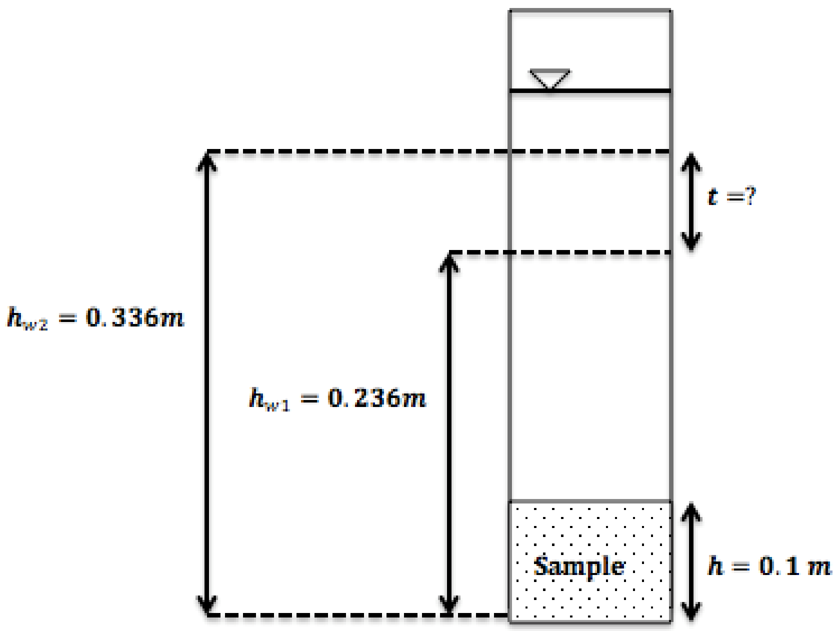

Figure 9. Systematic View of Permeability Test Apparatus

Since the flow velocities of water in measuring cylinder and soil samples are the same:

$$v_{sample} = \frac{k}{\gamma_{water}} \frac{u_{excess}}{h} = v_{cylinder} = -\frac{dh_{water}}{dt}$$

And $u_{excess} = h_{water}\gamma_{water}$, therefore:

$$\frac{k}{h} h_{water} = -\frac{dh_{water}}{dt} \Rightarrow$$

$$\int_{h_{w1}}^{h_{w2}} \frac{dh_{water}}{h_{water}} = \int_0^t -\frac{k}{h} dt \Rightarrow$$

$$k = \frac{h}{t} \ln \frac{h_{w1}}{h_{w2}} \qquad (15)$$

Here, $h = 0.1\ m, h_{w1} = 0.336\ m\ and\ h_{w2} = 0.236\ m$

Example for host sand: the average time measured is $t = 35.9\ s$, substitute these numbers into equation (15):

$$k_{hostun} = \frac{0.1}{35.9} \ln \frac{0.336}{0.236} = 0.000984\ {}^{m}/_{s}$$

4.2.2 ONE-DIMENSIONAL CYLINDER TEST

Figure 10 and Figure 11 show the test apparatus. The saturated soil samples are placed in the cylinders; thermocouples are attached to both ends of them, so the temperatures of both ends of the samples could be measured. The power input can be controlled by the power supply, and the height and cross-sectional area of the samples are fixed. The temperatures at each thermocouple are recorded each second and final readings will be taken when they reach steady state. One test cylinder has a hot plate on the top and the other has a hot plate at the bottom.

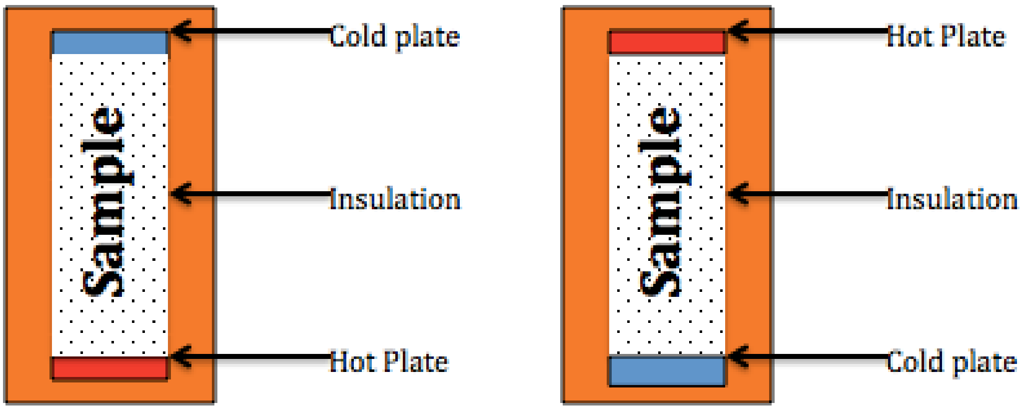

Figure. 10 Systematic Views of One-dimensional Test Apparatus

Figure 11. Actual View of One-dimensional Test Apparatus

If we look at the left cylinder in Figure 10 above, as the temperature at the bottom increases, the density of the water in the sample will become lower, so the water starts to move up which gives convection. For the other cylinder with hot plate on the top, there won't be any convection.

The amount of conduction is quantified by thermal conductivity, which is calculated as:

$$\lambda = \frac{QH}{A\Delta T} \qquad (16)$$

Q is the power in *W*

H is the length of the cylinder in *m*

A is the area of cross-sectional area in m^2

ΔT is the temperature difference between the ends of cylinder in *K*

Percentage convection can be calculated as:

$$\%\ Convection_{1D} = \frac{(T_{2t} - T_{2b}) - (T_{1b} - T_{1t})}{T_{2t} - T_{2b}} \qquad (17)$$

T_{1t} is the temperature at the top of the first cylinder

T_{1b} is the temperature at the bottom of the first cylinder

T_{2t} is the temperature at the top of the second cylinder

T_{2b} is the temperature at the bottom of the second cylinder

According to equation (5), *Nusselt* number can be calculated as:

$$Nu = \frac{T_{2t} - T_{2b}}{T_{1b} - T_{1t}} - 1 \qquad (18)$$

According to equation (7), *Rayleigh* number can be calculated as:

$$Ra = \frac{k(T_{1b} - T_{1t})H}{\lambda} \times \frac{C_p \alpha g}{v} \qquad (19)$$

In this case, H and A are fixed to 0.2 *m* and 0.00833 m^2.

4.2.3 TWO-DIMENSIONAL PIPE TESTS

Figure 12 shows a systematic view of the two-dimensional test apparatus. In two-dimensional tests, saturated soil samples are placed in a well insulated box, a cartridge heater is buried in the samples, one thermocouple is placed next to the heater, another is placed on the surface of the soil sample, and the temperatures at both location are recorded every second. Final readings are taken when they reach equilibrium. Hence, the temperature difference and all the dimensionless groups discussed in section 3.3 could be calculated.

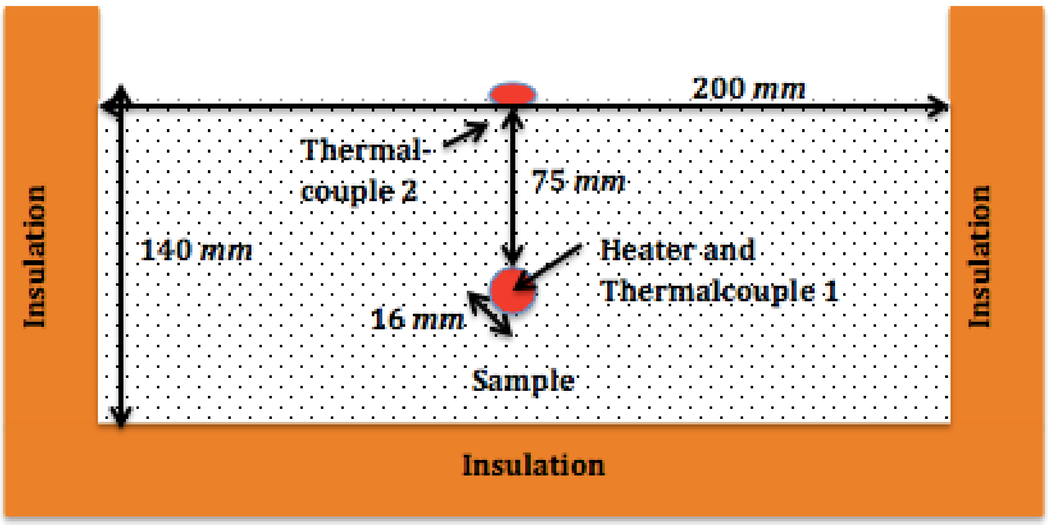

Figure 12. Systematic View of Two-dimensional Test Apparatus

In two-dimensional pipe tests, the amount of conduction could be quantified by dimensionless thermal conductivity, which could be calculated as:

$$\beta = \frac{QH}{LD\lambda(T_1 - T_2)} \qquad (20)$$

Q is the power applied to samples with units: W

H is the characteristic length with units: m

L is the length of the pipe/heater with units: m

D is the diameter of the heater with units: m

λ is the thermal conductivity with units: $Wm^{-1}K^{-1}$

T_1 is the temperature of thermocouple 1 with units: K

T_2 is the temperature of thermocouple 2 with units: K

Based on the definition of equation (5), Nusselt number can be calculated as:

$$Nu = \frac{\beta}{\beta_{conductive}} - 1 \qquad (21)$$

Where $\beta_{conductive}$ is the dimensionless conductive heat transfer coefficient, found from finite element analysis as described in section 4.2.4.

Based on the definition of equation (7), Rayleigh number could be calculated as:

$$Ra = \frac{k(T_1 - T_2)H}{\lambda} \times \frac{C_p \alpha g}{\nu} \qquad (22)$$

4.2.4 FINITE ELEMANT ANALYSIS OF CONDUCTION FROM A BURIED PIPE

ABCUS finite element analysis is used to determine the dimensionless conductive heat transfer coefficient, $\beta_{conductive}$. Figure 13 shows the analysis configuration:

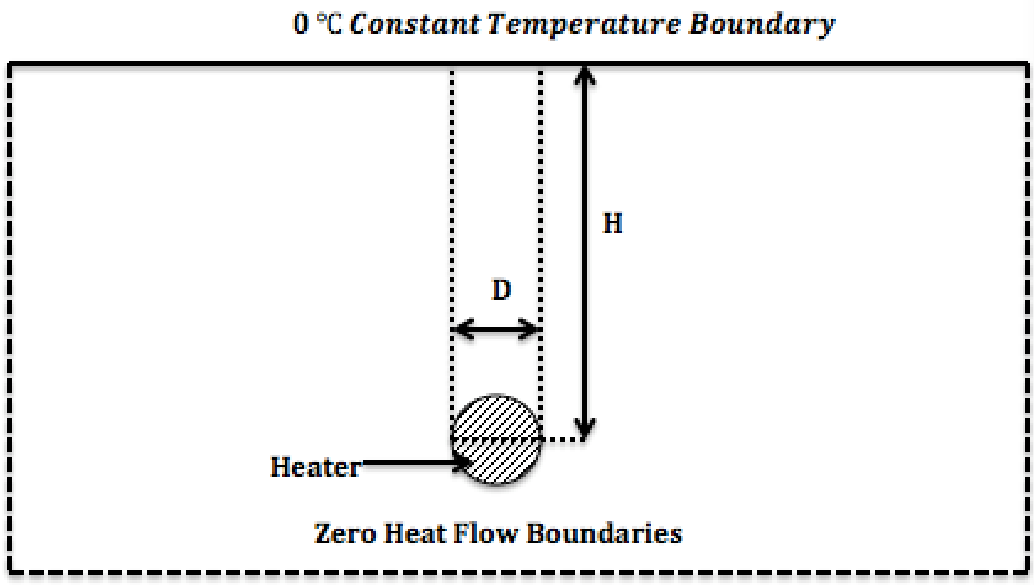

Figure 13. Finite Element Analysis Configuration

If the body heat flux from the heater is Q_{flux}, the temperature difference between the heater and $0\,°C$ *constant temperature boundary* is ΔT_{flux} and thermal conductivity λ is assumed to be 3 W/mK, therefore:

$$Q_{flux} = \frac{\lambda \Delta T_{flux} DL}{H} \qquad (23)$$

If heat is only transferred in the vertical column shown in Figure 13, then:

$$\frac{Q_{flux}H}{\lambda\Delta T_{flux}DL} = 1 \quad (24)$$

However, heat is transmitted in all directions, Figure 14 shows the flows of heat flux with arrows pointing the directions of flows:

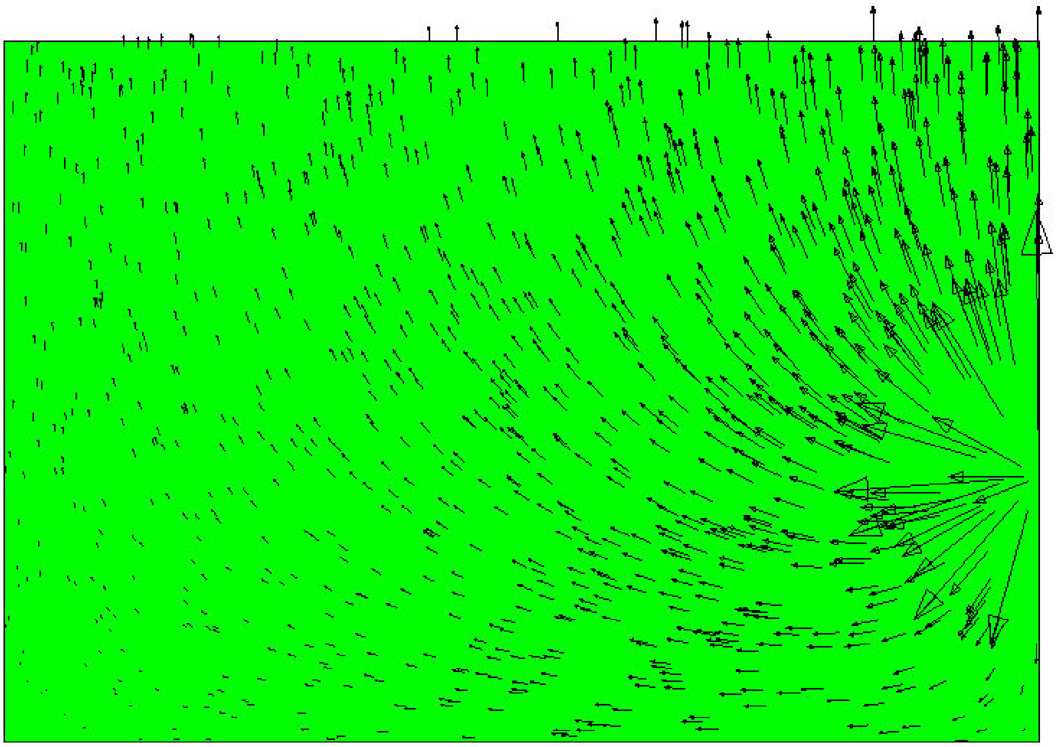

Figure 14. Flows of Heat Flux

Hence finite element analysis is used to obtain $\beta_{conductive}$ in real situation. The analysis was run under different geometries, i.e. different values of H/D. In this project H=0.075 *m*, D=0.015875 *m*, which gives H/D=4.72. The result obtained according to this specific geometry is:

$$\beta_{conductive} = 6.88 \quad (25)$$

Figure 15 shows the results of finite element analysis. Figure 16 shows the mesh of the analysis, which has a total of 32766 elements, and Figure 17 shows the temperature distribution.

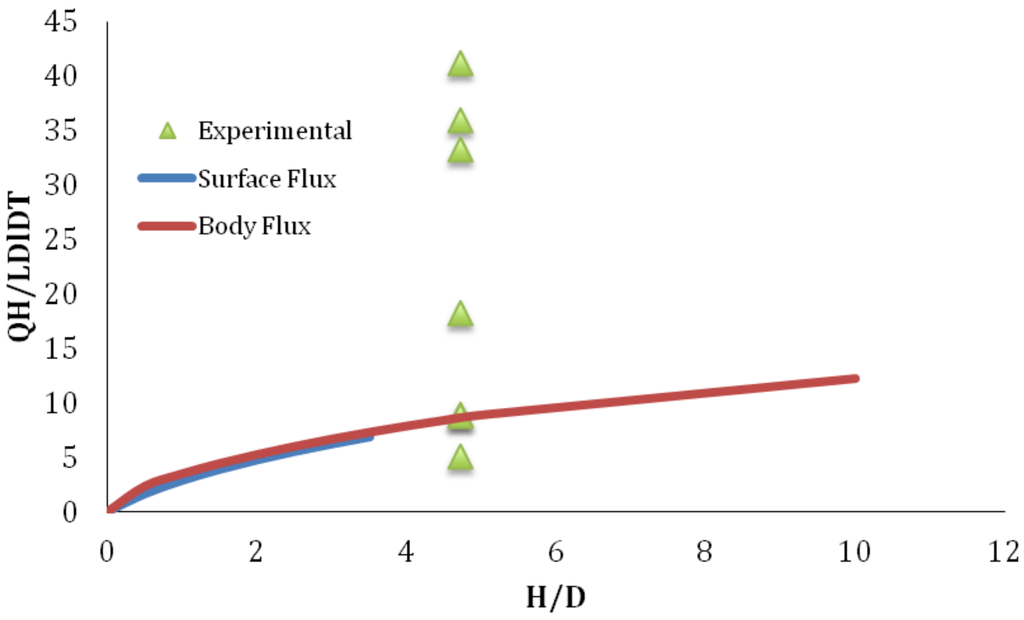

Figure 15. Results of Finite Element Analysis

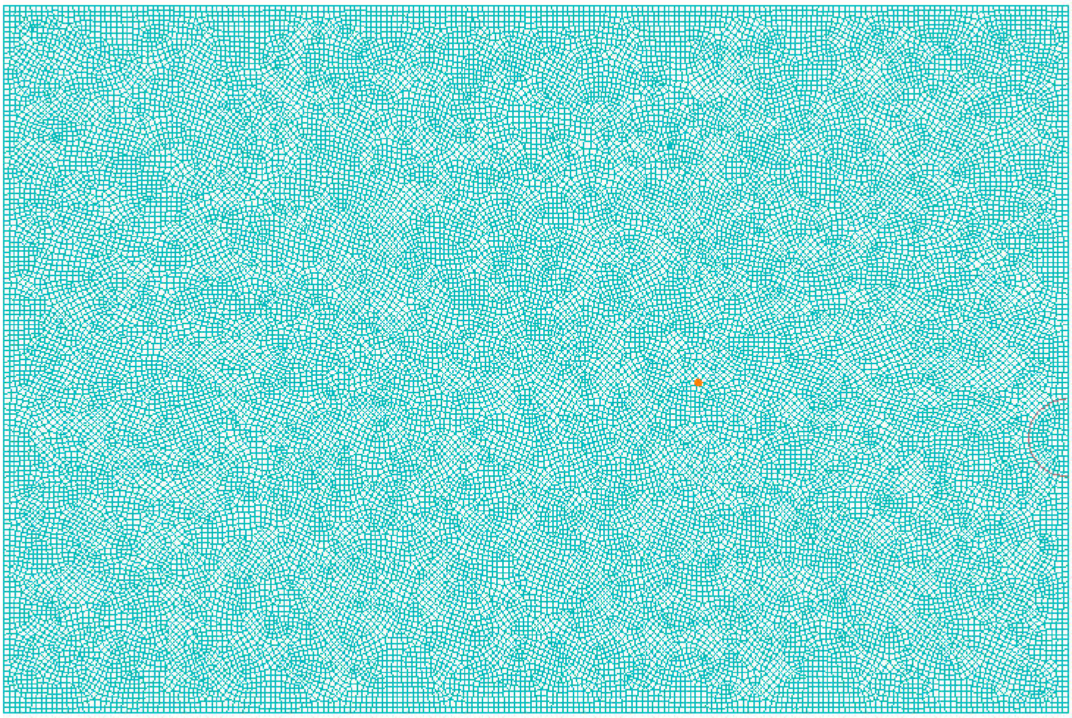

Figure 16. Mesh of Finite Element Analysis

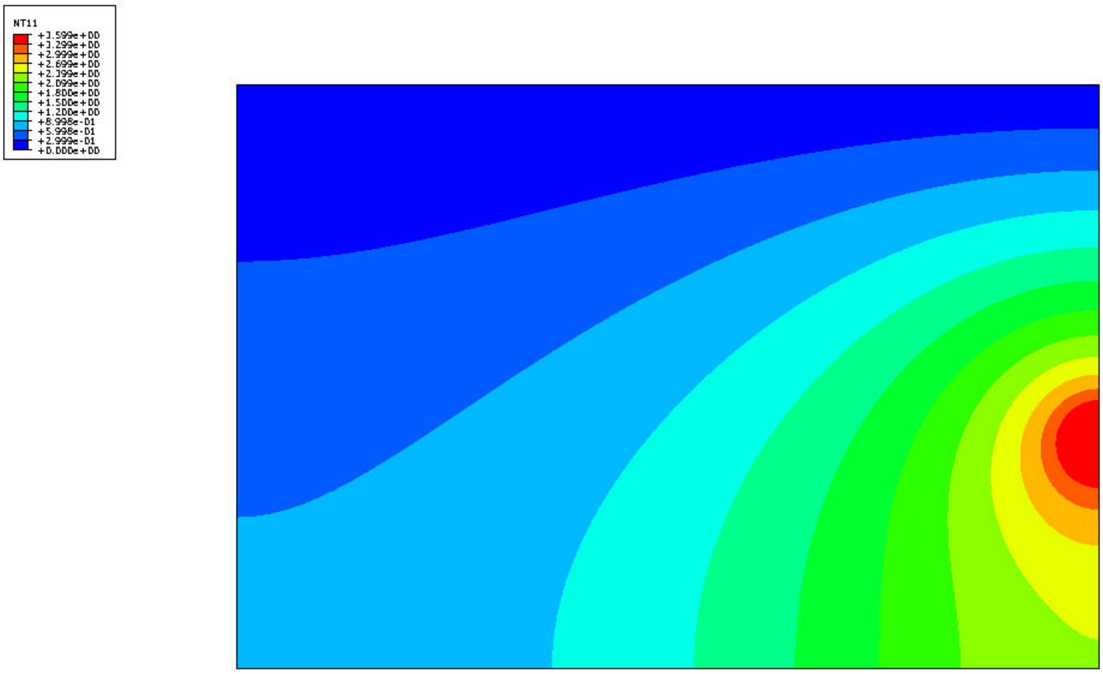

Figure 17. Temperature Distribution of Finite Element Analysis

5. EXPERIMENTAL RESULTS AND DISCUSSION

In this section results of both one-dimensional tests and two-dimensional tests are discussed.

5.1 ONE-DIMENSIONAL CYLINDER TEST RESULTS

One-dimensional tests results are shown and discussed below, including permeability test results, thermal conductivity, *Nu* number, *and Ra* number in each soil materials. All tests are carried out with a power of 5.75 W.

5.1.1 LAPWOOD'S THRESHOLD THEORY OF STEADY CONVECTION

Table 2. One-dimensional Test Results

Sample	k (m/s)	ΔT_{12} (°C) (hot at top)	ΔT_{34} (°C) (cold at top)	Conductivity λ (W/mK)	*Nu*	*Ra*
Hostun Sand	1×10^{-8}	33.14	37.01	4.10	0	10.66

Frac. B	3.5×10^{-3}	28.67	33.38	4.82	0	30.00
Frac. A	7×10^{-8}	27.85	24.66	4.87	0.129	41.72
Frac. A (17.8% of total mass)&Gravel (5 *mm*)	11×10^{-8}	36.73	19.18	3.76	0.915	72.02
Gravel (5 *mm*)	22×10^{-8}	39.30	14.28	3.51	1.752	109.39
Gravel (10 *mm*)	39×10^{-8}	45.22	16.67	3.05	1.713	261.19

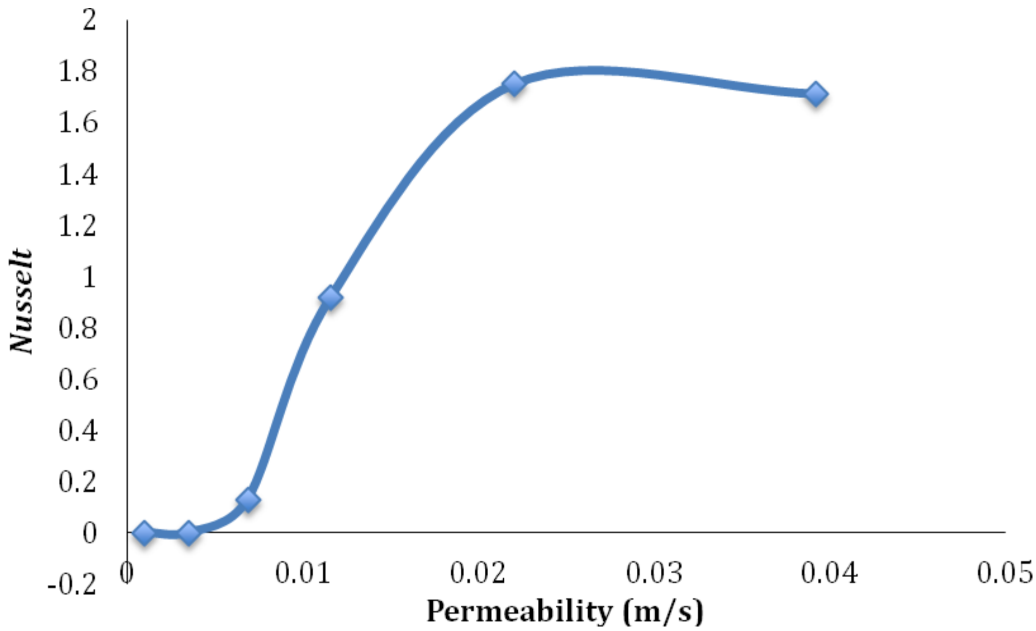

Figure 18. ***Nusselt*** **number vs. Permeability (5.75 *W*)**

In this problem the type of convective process is free convection, the temperature gradient causes density variations, which in turn results in liquid flow. Equation (8) shows that the magnitude of Rayleigh number is proportional to permeability, and Rayleigh number is used to quantify the amount of free convection in soil materials. From Figure 18 above we can see that, before *Ra* exceeds certain value, there is no steady convection that is because the values of permeability are too small, there will not be any continuous flow of water presents. As mentioned before, Lapwood (1948) said, the temperature gradient must exceed a threshold value for steady convection to become possible. And he quantifies the threshold value as:

$$\frac{\Delta T}{H} = \frac{4\pi^2 \lambda}{\rho C_p k \alpha H^2} \qquad (26)$$

Where ρ _D_Dd________ĝÿƧƧ__ C_p is volumetric heat capacity; α D_Dd________ÒĎƧƧ_____________(^)/ _D_Dd_____ is thermal conductivity; k (^)/ _D_Dd___

From equation (7) and (26), we get:

$$Ra = \frac{4\pi^2 g}{\rho m} \qquad (27)$$

Since $\rho = 1000\ kg/m^3$, and kinematic viscosity of water $\nu = 1.004 \times 10^{-6}\ m^2/s$ at $20℃$ 〖〗 ^_D_Dd________-ÿƧƧ__________.

From equation (26), we can see that low permeability values imply high threshold values, in the case of constant power rating, temperature gradients are more or less fixed, and small permeability will make threshold value too large for any steady convection to take place.

As soon as permeability exceeds the certain value for a particular power rating, the amount of convection in soils varies proportionally with permeability, which agrees with equation (8).

If permeability is fixed, and the power rating is variable, test results of the mixture of Gravels with an average diameter of 5 *mm* and Fraction A are:

Table 3. Gravel (5 *mm*) + Fraction A (17.8% of total mass) under various power ratings

Power (W)	$T_{2t} - T_{2b}$	$T_{1b} - T_{1t}$	Nu
1.08	9.56	10.54	0
1.45	12.25	11.62	0.0542
1.61	14.12	12.64	0.117
2.07	17.80	13.98	0.237
5.75	36.73	19.18	0.915

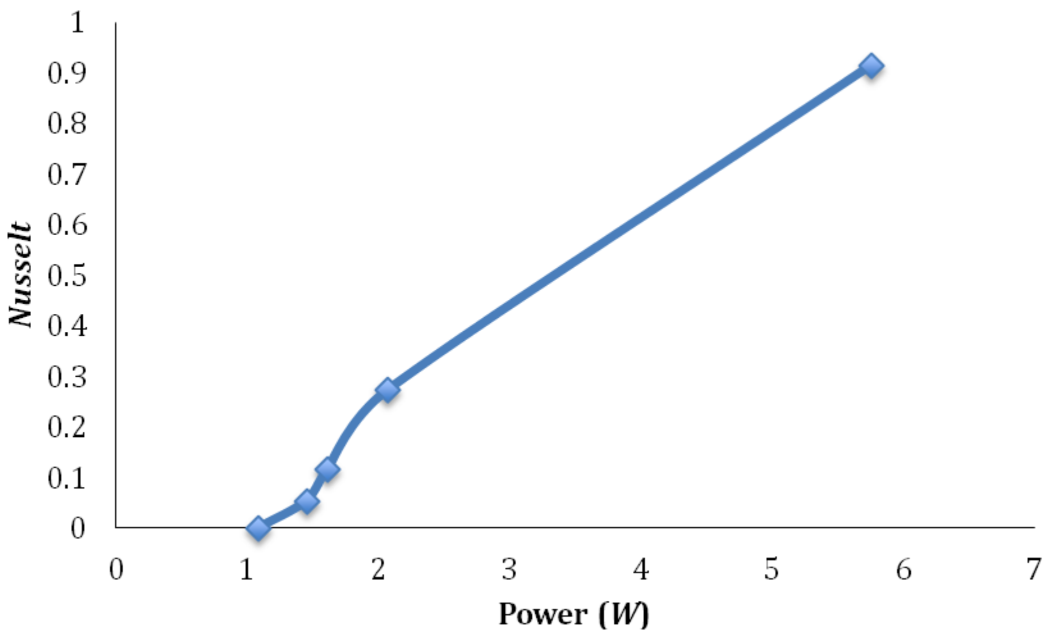

Figure 19. *Nusselt* vs. Power Rating [Gra. (5 *mm*) + Frac. A (17.8% of total mass)]

Figure 19 shows that before a certain value of power rating, in this case is about 1.08 *W*, there is no steady convection in the mixture. When power rating exceeds this value, steady convection becomes possible and the amount of convection varies almost linearly with power rating.

Above all, there is a good agreement between experimental results and the threshold theory of steady convection proposed by Lapwood (1948). Which is: the temperature gradient must be greater than a certain value for steady convection to become possible, otherwise, ant disturbance dies away, and this threshold value is inversely proportional to permeability.

5.1.2 NUSSELT NUMBER AND RAYLEIGH NUMBER

In this section, values of *Nusselt* number and *Rayleigh* number of various soil materials are calculated and compared, under both the same power rating and variable power supply. Table 4 shows values of both dimensionless numbers under the same power, which is 5.75 *W*. Table 5 shows values of *Nusselt* and *Rayleigh* number for various materials under different power supplies.

Table 4. *Nusselt* and *Rayleigh* values for soils under the same power rating (5.75 *W*)

Sample	*Nu*	*Ra*
Hostun	0	10.656
Fraction B	0	29.995
Fraction A	0.129	41.721
Grav. (5 *mm*)+Frac. A (17.8% of total mass)	0.915	72.017
Gravel (5 *mm*)	1.752	109.390
Gravel (10 *mm*)	1.713	261.194

From the table above we can see that *Nusselt* number of Gravel (5 *mm*) with Fraction A (17.8% of total mass) is close to one, which means the magnitudes of convection and conduction are of similar order, conduction dominates in soil materials with particle sizes smaller than that and convection dominates in soils with particle sizes larger than that.

Rayleigh number is another way to compare the relative magnitudes of conduction and convection. Before *Rayleigh* number exceeds a critical number, conduction dominates; otherwise convection plays a more important role.

As it is shown below, *Nusselt* number is linearly proportional to *Rayleigh* number up until *Rayleigh* number around 110, after that *Nusselt* number does not vary much with the increasing *Rayleigh* number, which means even the amount of convection presents in the soils keeps increasing, the relative magnitude between conduction and convection does not change a lot. That is because for fine materials, conduction dominates, however, as the particle sizes increases, moisture content increases as well, therefore, convection becomes more and more important, eventually, there is a point (a certain type of soil, either pure or mixture) where the amounts of conduction and convection are about the same.

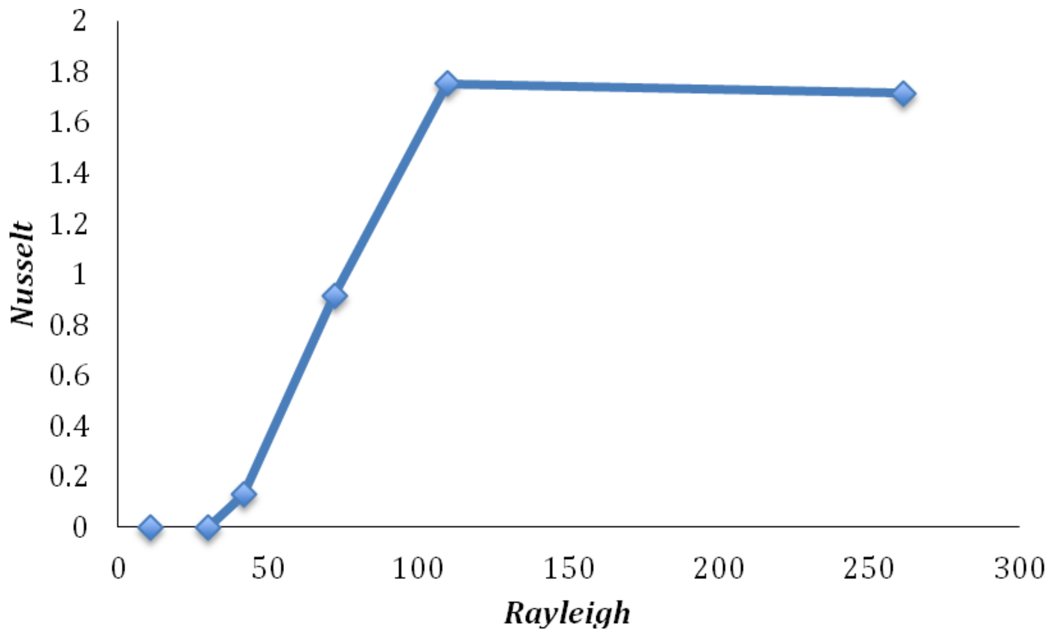

Figure 20. ***Nusselt*** **number against** ***Rayleigh*** **number**

The above observations are all based on constant power rating; hence, it is necessary to examine the effects of variable powers settings on soil materials. Table 4 below summarises values of *Nusselt* number and *Rayleigh* number of Gravels (5 *mm*) + Fraction A (17.8% of total mass) sand under various power ratings:

Table 5. Values of ***Nu*** **and** ***Ra*** **of Gravels (5** ***mm*****) + Fraction A sand (17.8% of total mass) under various power ratings**

Sample	Power (*W*)	*Nu*	*Ra*
Grav. (5 *mm*)+Frac. A	1.08	0	54.813
	1.45	0.0542	57.704
	1.61	0.117	65.146

(17.8% of total mass)	2.07	0.273	70.662
	5.75	0.915	72.017

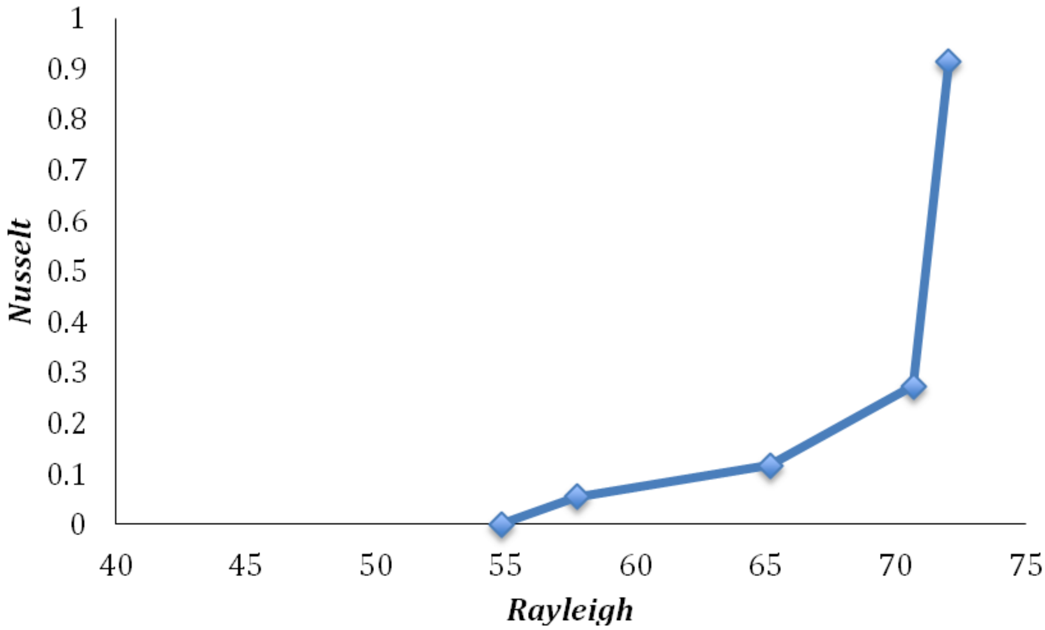

Figure 21. ***Nusselt*** **vs.** ***Rayleigh*** **of Gravel (5** ***mm*****)+Frac. A**

A few *Nusselt* values from actual measurements are zero, which simply means no steady convection in the samples, in those cases *Nusselt* number are taken to be zero.

We can see that both *Nusselt* and *Rayleigh* numbers are proportional to power rating (temperature gradient). Initially, *Nusselt* number is zero shows no steady convection in the sample, as temperature gradient keeps increasing, steady convection may become possible. From Figure 21 above, the threshold value of *Rayleigh* number for stable convection is between 55 and 57 for this particular soil sample. More data points need to be taken to determine the accurate value of critical *Rayleigh* number

Above all, in the fist set of experiments, it is shown that the amount of heat transfer by convection is strongly dependent on the permeability of soils.

When the permeability is low, conduction is the primary heat transfer mechanism, as the amount of pore water increases, convection becomes more and more important, and eventually reaches a point where convection dominates. This result agrees with Figure 5 above, in these experiments, all soil samples are fully saturated, as the particle size increases, the dominating transfer mechanism changes from conduction to convective heat transfer in water. In the second set of tests, particle size is fixed and power rating is changed, which implies a variable temperature gradient, the results show that the amount of convection present is also proportional to the temperature gradient.

5.2 TWO-DIMENSIONAL BURIED PIPE TEST RESULTS

In this section, the results of two-dimensional buried pipe tests are shown; values of *Rayleigh* number are calculated directly from measurements using equation (7) above. The thermal conductivities calculated in these experiments include both effects of conduction and convection heat transfer, thus the dimensionless thermal conductivities calculated can be taken as the $total\ heat\ transfer\ coefficient$ in equation (5), and $conductive\ heat\ transfer\ coefficient$ is discussed in section 4.2.4. Please see Table 6 below for two-dimensional test results

Table 6. Two-dimensional Test Results

Sample	Power (*W*)	*Nu*	*Ra*
Hostun	1.92	0.361	0.719
	8.25	0.0635	3.96
	16.1	-0.0487	8.63
	0.175	-0.433	6.27
	1.50	0.00586	30.3
	2.16	-0.0102	44.4

Gravel (10 *mm*)	2.84	1.05	28.1
	6.00	2.74	32.7
	8.64	3.05	43.4
	11.8	3.63	51.7
Grav. (5 *mm*)+Frac. A (5% of total mass)	5.7	5.00	7.91
	7.88	-0.153	77.4
Grav. (5 *mm*)+Frac. B (5% of total mass)	5.7	28.1	1.29
	7.88	21.2	2.35
Grav. (5 *mm*)+Frac. A (47.8% of total mass)	8.375	0.113	26.8
	12.3	0.360	32.3
	18	0.890	34
Grav. (5 *mm*)+Frac. B (45% of total mass)	8.375	0.272	12.1
	12.3	0.401	16.2
	18	0.845	18

Some of the *Nusselt* values are negative in Table 6 above, theoretically, *Nusselt* number should be positive. Here, negative value means no convective heat transfer in soil materials.

According to Lapwood (1948), the values of critical *Rayleigh* number are: for conducting boundaries-impervious below and free surface above, $Ra_c = 27.1$. For impervious conducting boundary below and free surface with imperfect conduction above: $Ra_c = 39.5$.

For Hostun sand, the magnitude of *Nusselt* number is inversely proportional to power. As power supply increases, *Rayleigh* number increases (but still well below the critical *Rayleigh* number for steady convective flow), which means the absolute amount of heat convection increases, however, since *Nusselt* number drops, the relative amount of convection compared to conduction decreases. Therefore, the rate of increase of conduction is greater than that of convection in fine materials such as Hostun sand. The reason is as soil particles are so close to each other, the majority heat energy will be transferred via conduction, and only a small part of heat will be transferred by convection due to low permeability. As power keeps rising, *Nusselt* number goes below zero, indicates no steady convection at all. Actually, no matter how large is the temperature gradient (power); there will not be any steady convection present in Hostun sand.

Figure 22 shows *Nusselt* number against *Rayleigh* number of Gravels with an average diameter of 10 *mm*.

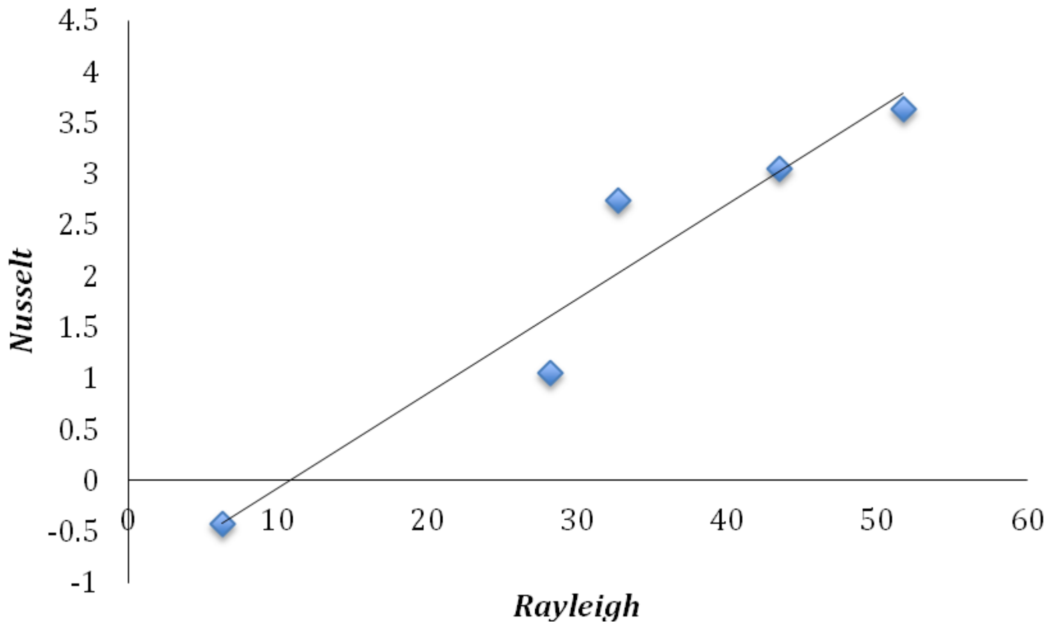

Figure 22. Nusselt vs. Rayleigh number of Gravel (10 *mm*)

For coarse materials like Gravels, most *Rayleigh* number values exceed the critical value of 27.1, thus, steady flow of convection is possible since the temperature gradient is large enough. As temperature gradient increases, *Nusselt* number increases generally shows convective heat transfer becomes more and more important; as soon as it exceeds one, convection becomes the dominating heat transfer mechanism. As it is shown in Figure 22 above, it seems that there is a linear relationship between *Nusselt* number and *Rayleigh* number. Therefore, if enough data points are taken and they still follow a linear relationship, one of the dimensionless numbers could be used to predict another using the best-fit line.

For mixtures, their behaviour is dominated by finer soils in them, i.e. Fraction A sand and Fraction B sand. The permeability of Gravel (5 *mm*) + Fraction A and Gravel (5 *mm*) + Fraction B are 0.01606 *m/s* and 0.01273 *m/s* respectively, which are significantly lower than that of Gravel (5 *mm*) (0.022 *m/*s) alone, even though the mass fractions of Fraction A and Fraction B are only 5%. The *Rayleigh* number values of Hostun sand and Gravel (5 *mm*) + Fraction B mixture are of the same order while those of Gravel (5 *mm*) + Fraction A mixture are closer to values of Gravel (10 *mm*), which again shows finer materials determines the overall properties of the mixtures. Hence, the trends of *Nusselt* and *Rayleigh* numbers of those two mixtures will be similar to those of Hostun sand.

Another set of mixtures has also been tested under various powers, which are Gravel (5 *mm*) + Fraction A (47.8% of total mass) and Gravel (5 *mm*) + Fraction B (45.0% of total mass). The magnitudes of *Rayleigh* number of the two mixtures are in the same order, but under the same power ratings, the mixture with Fraction A sand has higher *Rayleigh* values. Fraction B sand is much finer than Fraction A, hence, permeability in the mixture is lower, which makes it more difficult for water to seep through, so less heat convection occurs in the mixture.

6. CONCLUSION

The magnitudes of heat transfer by conduction, convection, thermal radiation and water vapour diffusion depend on several factors including: particle size, temperature gradient and saturation level. Different values of these factors will lead to different dominating heat transfer mechanisms.

In highly saturated soil materials with small average particle size, conductive heat transfer plays the most important role. Examples are clay and silt. Since the soil particles are so small, the permeability is low, therefore, it is almost impossible for water to migrate through those fine soil particles, so convective heat transfer in water could be neglected even the temperature gradient is high. As the soils are highly saturated, which means little air in the pores, hence there is no convective heat transfer in air presents. Water vapour diffusion strongly depends on moisture content, and could also be ignored due to low volumetric water content. The magnitude of thermal radiation is proportional to particle size and pore cross-sectional area. In the case of small average particle size and low voids ratio, the effect of thermal radiation could be ignored. Above all, conduction becomes the dominating heat transfer mechanism in highly saturated soils with small average particle size.

As particle size increases, permeability increases, and then steady water migration becomes possible. Since the soils are still highly saturated, there is no heat convection in air. If the temperature gradient is large enough for *Rayleigh* number to exceed its critical value, convective heat transfer in water will be the dominating heat transfer mechanism.

For moderately saturated soils with small average particle size, temperature-dependent vapour diffusion becomes important; it contributes during the processes of vaporization and condensation. As particle size increases, thermal radiation in voids comes next, its magnitude depends on voids ratio and temperature level.

For soils with low saturation level and small average particle size, moisture-dependent water vapour diffusion becomes important. Moisture content gradient causes water vapour diffusion due to change in relative humidity, and large variations of relative humidity only happen at low saturation levels. In this region, depends on the temperature level, water vapour diffusion could also occur in the pore air. For soils with larger particle sizes, such as coarse sand and gravels, air content is much large than fine materials due to low saturation level and larger voids ration, convective heat transfer in air also becomes important.

In this project, different soil combinations have been tested under various powers. Since all the samples are fully saturated only heat conduction and convection are considered, temperature differences are measured and thermal conductivities are calculated, therefore, *Nusselt* number and *Raylieigh* number could be obtained from those calculated results, and are compared for different materials. The relationships between particle size, temperature level and dominating heat transfer mechanisms have been verified and discussed, which are: magnitude of convective heat transfer is proportional to particle size and temperature gradient, while the magnitude of conductive heat transfer is proportional to temperature level and inversely proportional to particle size. The threshold effect of steady heat convection is also discussed in section 5.1.1.

7. RECOMMENDATION

In this section, both recommendations for current development and future work are given.

7.1 RECOMMENDATIONS FOR CURRENT DEVELOPMENT

In the project, all soil samples are tested under fully saturated condition; therefore, heat transfer mechanisms have been limited to only heat conduction and convection. Next step, different saturation levels should be tested, therefore, the relationship between particle sizes, temperature levels and other heat transfer mechanisms could be explored.

In one-dimensional cylinder tests and two-dimensional pipe tests, the characteristic lengths are fixed, which are 0.2 *m* and 0.075 *m* respectively, so various sample heights should be used.

Nusselt-Rayleigh relationship depends on soil geometry and other external conditions, such as the presence of external heat sources and pump systems. It is well known that the power-law index of the *Nusselt-Rayleigh* numbers relationship is around 1/3 (Christensen, 1984), which is predicted by the boundary layer theory of the box model without internal heating (Turcotte and Oxburgh, 1967). However, a power-law index of 1/4 has been reported for spherical geometry models (Ratcliff, Schubert and Zebib, 1996). In order to get an accurate *Nusselt-Rayleigh* relationship for various samples, a more powerful power supply could be used; so more data points for each soil sample could be taken and the relationship between *Nusselt* number and *Rayleigh* number can be further investigated.

7.2 PROPOSALS FOR FUTURE WORK

All the measurements and analysis done so far are under ideal condition, i.e. no external influences such as heat sources or pumps. However, in the real world, soil thermal properties could be affected by many other factors. For examples, thermal properties of soils around undersea oil pipelines may well be affected by ocean waves. While in farmlands they may be changed by pumping activities and solar radiation. It is important to include these external sources to the analysis so the data obtained could be applicable to real situations.

8. NOMENCLATURE

8.1 ROMAN LETTER SYMBOLS

Nu: *Nusselt* number, dimensionless

Ra: *Rayleigh* number, dimensionless

e: voids ratio, dimensionless

V: volume, m^3

n: porosity, dimensionless

P: partial pressure, *Pa*

P_w^* : saturated vapour pressure, *Pa*

u: volumetric flow rate, m^3s^{-1}

Q: power, *W*

H: characteristic length, *m*

L: length of pipe/heater, *m*

D: diameter of heater, *m*

ΔT : temperature difference, *K*

A: area, m^2

g: gravitational acceleration, ms^{-2}

k: permeability, ms^{-1}

C_p : volumetric heat capacity, $Jm^{-3}K^{-1}$

∇P_w : vapour pressure gradient, *Pa*

q: amount of heat transferred, *J*

D_a : water vapour diffusion coefficient, m^2s^{-1}

r: latent heat due to vaporisation of water, $KJkg^{-1}$

R: universal gas constant, $JK^{-1}mol^{-1}$

v: velocity, ms^{-1}

t: time, *s*

h: height of water, *m*

γ : flow flux, m^2s^{-1}

8.2 GREEK LETTER SYMBOLS

β : dimensionless thermal conductivity

θ : volumetric water content, dimensionless

φ : relative humidity, dimensionless

λ : thermal conductivity, $Wm^{-1}K^{-1}$

α : volumetric thermal expansion coefficient of water, K^{-1}

λ^* : apparent air conductivity, $Wm^{-1}K^{-1}$

ν : kinematic viscosity, m^2s^{-1}

8.3 SUBSCRIPTS

w: water

s: solid

T: total

v: vapour

a: air o: total pressure

9. REFERENCE:

Asrar, G., and Kanemasu, E. T. (1982): Estimating thermal diffusivity near the soil surface using Laplace transforms: Uniform initial conditions. Soil. Sci. Soc. Am. J. 47. p397-401.

Bristow, K. L., Kluitenberg, G. J., Goding, C. J., Fitzgerald, T. S. (2001): A small multi-needle probe for measuring soil thermal properties, water content and electrical conductivity. *Computers and Electronics in Agriculture* 31 (3): p265–280.

Cary, J. W. (1965): Water flux in moist soil: Thermal versus function gradients. Soil Science. -CO, (3) p. 168-175.

Chen, S. X. (2008): Thermal conductivity of sands. Heat Mass Transfer 44, p1241-1246.

Christensen, U. R. (1984): Heat transport by variable viscosity convection and implications for the Earth's thermal evolution, Phys. Earth planet. Inter., 35, p264-282.

Clarke, B. G. Agab, A. and Nicholson, D. (2007): Model specification to determine thermal conductivity of soils. Geotechnical Engineering 161 Issue GE3. p161.

De Vries, D. A. (1963): Thermal properties of soils. Physics of the Plant Environment, W.R. Van Wijk, ed., John Wiley and Sons, p210-235.

Ewing, R. P., Horton, R. (2007): Thermal conductivity of a cubic lattice of spheres with capillary bridges. J. Phys. D: Appl. Phys. 40, 4959-4965

Gao, Z. Q., Fan, X. A. and Bian, L. G. (2003): An analytical solution to one-dimensional thermal conduction-convection in soil.

Gemant, A. (1950): The thermal conductivity of soils. J. Appl. Phys. 21, 750-752

Haigh, K. S. (2012): Thermal Conductivity of Sands. 11-P-043, University of Cambridge.

Home Footprint: http://www.homefootprint.info/GeoThermalEnergy.aspx

Horton, R., Wierenga, P. J. and Nielsen, D. R. (1983): Evaluation of methods for determining of apparent thermal diffusivity of soil near the surface. Soil Sci. Soc. Am. J. 47:23-32.

Johansen, D. (1975): Thermal property of soil. Ph.D. Thesis, Trondheim University.

Joshua, W. D. De Jong, E. (1973): Soil Moisture Movement under Temperature Gradients, Can. J. Soil. Scie. 53, p. 49-57.

Johansen, O. (1977): Thermal conductivity of soil. Corps of Engineers, U.S. Army. Cold Regions Research and Engineering Laboratory. Hanover, New Hampshire.

Kavianipoor, A., and Beck, J. V. (1977): Thermal property estimation utilizing the Laplace Transform with application to asphaltic pavement. Int. J. Heat Mass Transfer. 20:259-267.

Kim, J. et al. (2000): Energy partitioning and its imbalance over a prairie site in central Tibetan plateau during GAPE-IOP, 1998.

Kim, J., Hong, J., Gao, Z., and Choi, T. (2000): Can we close the surface energy budget in the Tibetan plateau? p13-16.

Krischer, O. (1934): Die Leitfahigkeit des Erdbodens. Beiheft zum Gesundheits-Ingenieur, Reihe I Heft 33, Munchen (Munich).

Krischer, O., Esdorn, H. (1940): Warmeleitung und Dampdiffusion in feuchten Gutern. VDI-Forsch,-Heft 402, Berlin.

Lapwood, E. R. (1948): Convection of a fluid in a porous media. Department of Geodesy and Geophysics Cambridge. p508-521.

Nagai, H., Kobayashi, T. and Ishikawa, H. (2000): An analysis of the land surface hydrological processes at the Amdo Station of GAME/Tibet using the BBH model.

National Statistics, Department of Energy & Climate change: DECC Publications: Energy Consumption in the UK: Domestic Data Tables 2011.

National Statistics, Department of Energy & Climate Change, DECC Publications: Energy Consumption in the UK: Overall Data Tables 2011.

Pacific Northwest National Laboratory, 2009: http://www.pnl.gov/science/highlights/highlight.asp?id=537

Passerat de Silans, A. M. B., Monteny, B. A. and Lhomme, J. P. (1996): Apparent soil thermal diffusivity: A case study. HAPEX-Sahel experiment. Agric. For. Meteorol. 81:201-216.

Philip, J. R., De Vries, D. A. (1957): Moisture movement in porous materials under temperature gradients. Transactions American Geophysical Union, 38, (2), p222-232.

Ratcliff, J. T., Schubert, G. and Zebib, A. (1996): Steady tetrahedral and cubic patterns of spherical-shell convection with temperature-dependent viscosity. J. Geophys. Rex, 101, p25473-25484.

Ren, T., Kluitenburg, G. J., Horton, R. (2000): Determining soil water flux and pore water velocity by a heat pulse technique. Soil Sci. Am. J. 64:p552-560.

Rollins, H. L. *et al.* (1954): Movement of Water in Soil due to a Temperature Gradient, Highway Research Board Proc. 33, p. 492-508.

Shao, M., Horton, R. and Jaynes, D. B. (1998): Analytical solution for one-dimensional heat conduction-convection equation. Soil Sci. Am. J. 62:123-128.

Smith, W. O. (1939): Thermal Conductivities in Moist Soils. Soil Sci. Soc. Am. Proc.

4, pp. 32-40.

Turcotte, D. L., Oxburgh, E. R. (1967): Finite amplitude convection cells and continental drift, J. Fluid Mech., 28, p29-42.

Van Wijk, W. R. (1963): Physics of Plant Environment. North Holland, Amsterdam.

10. APPENDIX

Please Table 7 and Table 8 below for both full one-dimensional and two-dimensional test results.

Table 7 Full One-dimensional Test Results

Sample	ΔT down (K)	ΔT up (K)	Q (W)	λ ($Wm^{-1}K^{-1}$)	k $\left(\frac{m}{s}\right)\times$	*Ra*	*Nu*
Hostun	33.1	37.0	5.75	4.16	9.84	10.7	0
Frac. B	28.7	33.4	5.75	4.81	35.5	30.0	0
Frac. A	16.7	17.9	2.8	4.02	68.8	37.3	0
	31.3	29.7	5.23	4.02	68.8	62.0	0.0534
	27.8	24.7	5.75	4.96	68.8	41.7	0.129
Grav. (5 *mm*)+Frac. A	9.56	10.5	1.08	2.71	116	54.8	0
	12.3	11.6	1.45	2.84	116	57.7	0.0542
	14.1	12.6	1.61	2.74	116	65.1	0.117

	17.8	14.0	2.07	2.79	116	70.7	0.273
	36.7	19.2	5.75	3.76	116	72.0	0.915
Grav. (5 *mm*)	8.94	10.1	1.08	2.90	221	93.8	0
	17.0	12.9	2.07	2.93	221	118	0.320
	25.3	12.8	3.68	3.49	221	98.7	0.978
	39.3	14.3	5.75	3.51	221	109	1.75
Grav. (10 *mm*)	45.2	16.7	5.75	3.05	393	261	1.71

Table 8. Full Two-dimensional Test Results

Sample	**Q (*W*)**	$k\ (\frac{m^2}{s}) \times 10^{-4}$	ΔT **(*K*)**	β	***Ra***	***Nu***
Hostun	1.92	9.84	1.5	12.1	0.719	0.361
	8.25	9.84	8.25	9.45	3.96	0.0635
	16.1	9.84	18	8.45	8.63	-0.0487
Grav. (10 *mm*)	0.175	393	0.328	5.04	6.27	-0.433
	1.5	393	1.59	8.94	30.3	0.00586
	2.16	393	2.32	8.79	44.4	-0.0102
	2.84	393	1.47	18.2	28.1	1.05
	6.00	393	1.71	33.2	32.7	2.74
	8.64	393	2.27	36.0	43.4	3.05

	11.8	393	2.70	41.1	51.7	3.63
Grav. (5 *mm*)+Frac. A (5%)	5.7	161	1.01	53.3	7.91	5.00
	7.88	161	9.89	7.53	77.4	-0.153
Grav. (5 *mm*)+Frac. B (5%)	5.7	127	0.208	259	1.29	28.1
	7.88	127	0.378	197	2.35	21.2
Grav. (5 *mm*)+Frac.A (47.8%)	8.38	68.8	8.00	9.89	26.8	0.113
	12.3	68.8	9.62	12.1	32.3	0.360
	18	68.8	10.1	16.8	34.0	0.890
Grav. (5 *mm*)+Frac. B (45%)	8.38	35.5	7.00	11.3	12.1	0.272
	12.3	35.5	9.34	12.4	16.2	0.401
	18	35.5	10.4	16.4	18.0	0.845